

## Electronic Supplementary Information:

### A Solid-State Electrolyte Based on Electrochemical Active $\text{LiMn}_2\text{O}_4$ for Lithium Metal Batteries

Jingzhen Du <sup>a</sup>, Zhichao Chen <sup>a</sup>, Bohao Peng <sup>b</sup>, Zewen Sun <sup>a</sup>, Wenzhuo Wu <sup>c</sup>, Qi Zhou <sup>b</sup>, Shuang Xia <sup>a</sup>, Lili Liu <sup>a,\*</sup>, Lijun Fu <sup>a</sup>, Yuhui Chen <sup>a</sup>, Tao Wang <sup>b</sup>, and Yuping Wu <sup>a,b,c,\*</sup>

<sup>a</sup> School of Energy Science and Engineering, Nanjing Tech University, Nanjing 211816, China

<sup>b</sup> Confucius Energy Storage Lab, School of Energy and Environment & Z Energy Storage Center, Southeast University, Nanjing 211189, China

<sup>c</sup> R & D Center, DKJ New Energy Materials Ltd. Co., Shaoxing 312365, China

## Materials

All of the chemicals mentioned in the synthesis steps were used directly without further treatment.  $\text{LiMn}_2\text{O}_4$  (LMO) was purchased from Tmall. Ltd. Electrolyte (LB-315) was purchased from Zhangjiagang Guotai Huarong New Chemical Materials Co., Ltd. The anodes (lithium foils) were purchased from Guangdong Canrd New Energy Technology Co., Ltd. Poly(vinylidene difluoride) (PVDF), *N*-methyl pyrrolidone (NMP), dimethylacetamide (DMAc) and acetylene black were purchased from Sinopharm Group Co., Ltd.

## Calculation

The ionic conductivity ( $\sigma$ ) and activation energy ( $E_a$ ) at different temperatures can be calculated from the following equation:

$$\sigma = \frac{L}{RS} = A \exp\left(\frac{-E_a}{K_B T}\right) \quad (\text{S1})$$

where  $L$  is the electrolyte thickness,  $R$  is the bulk resistance,  $S$  is the contact area of the SSE and electrode,  $K_B$  is the Boltzmann constant,  $A$  is the pre-exponential factor, and  $T$  is the temperature.

The lithium ion transfer number ( $t_{\text{Li}^+}$ ) was obtained through calculation from the following equation:

$$t_{Li^+} = \frac{I_s(\Delta V - I_0 R_0)}{I_0(\Delta V - I_s R_s)} \quad (S2)$$

where  $I_0$  and  $I_s$  are the initial current and steady-state current in the current curve respectively,  $\Delta V$  is the transition potential (10 mV),  $R_0$  and  $R_s$  are the AC impedance of the cell before and after polarization, respectively.

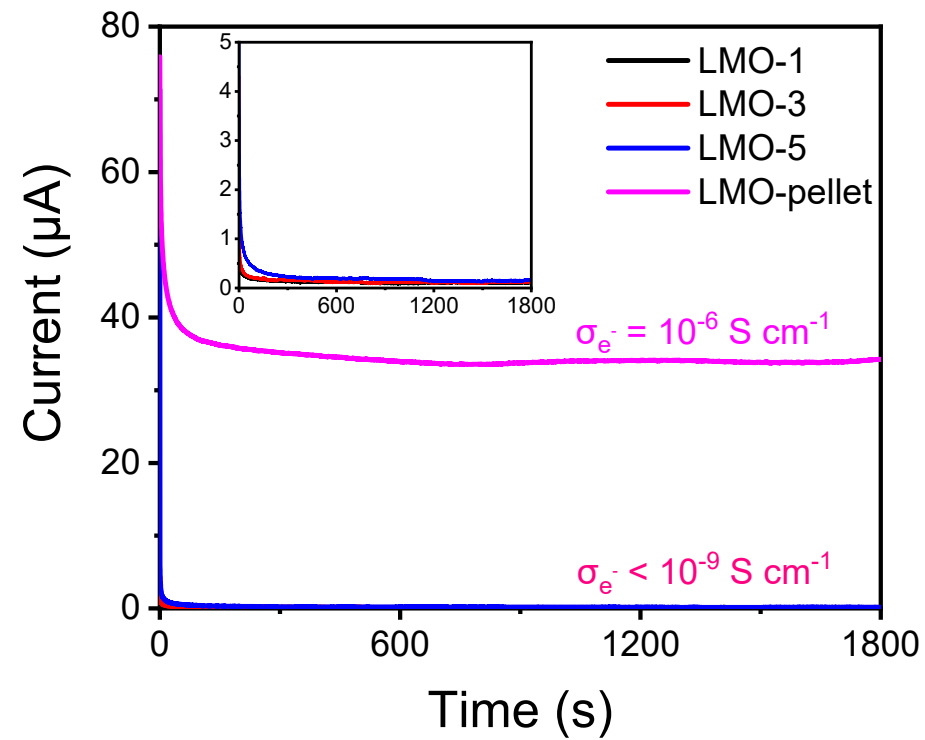


Figure S1. Chronoamperometry curve of electronic conductivity of LMO-X SSEs under 0.5 V.

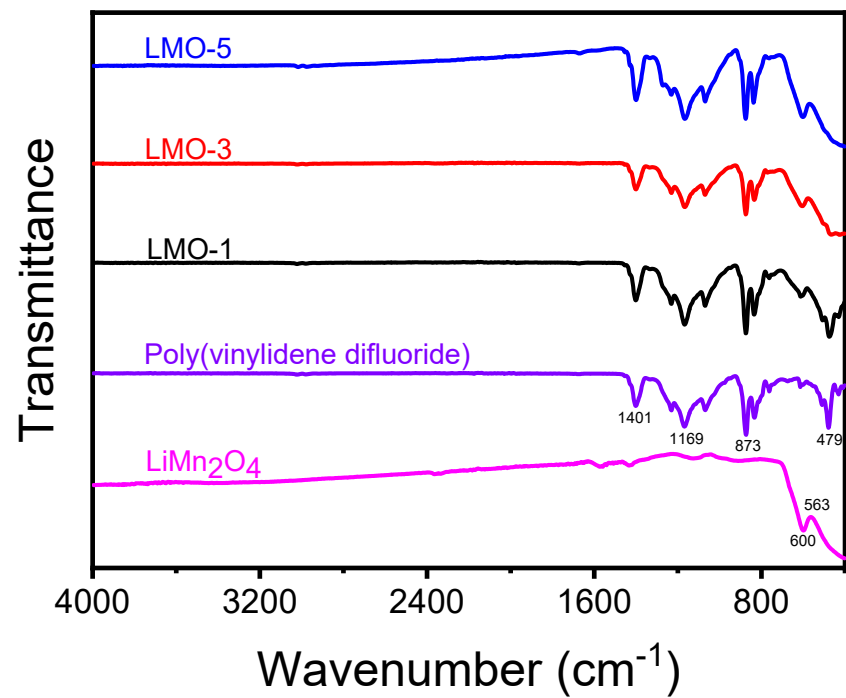


Figure S2. ATR-FTIR spectra comparison of LMO-X SSEs.

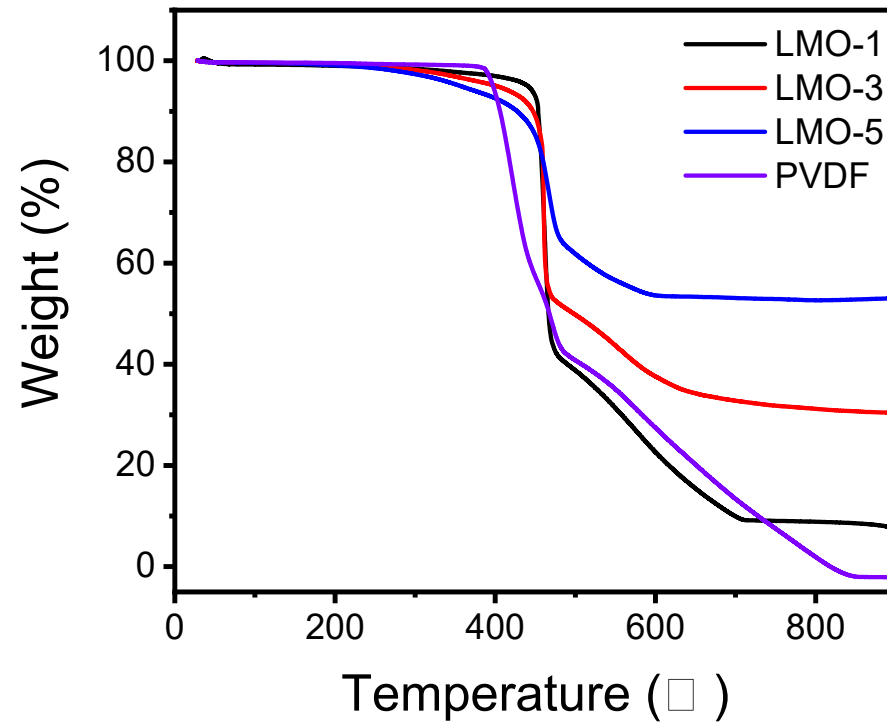


Figure S3. TGA image of LMO-X SSEs.

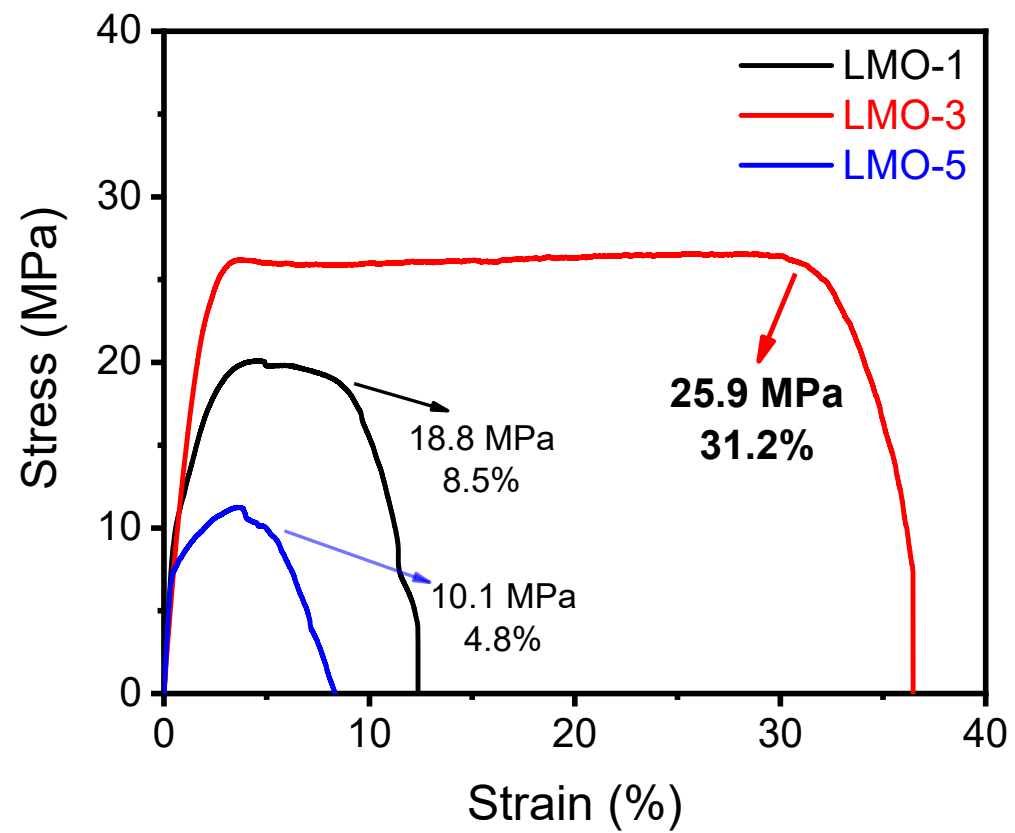


Figure S4. The stress-strain curves of LMO-X SSEs.

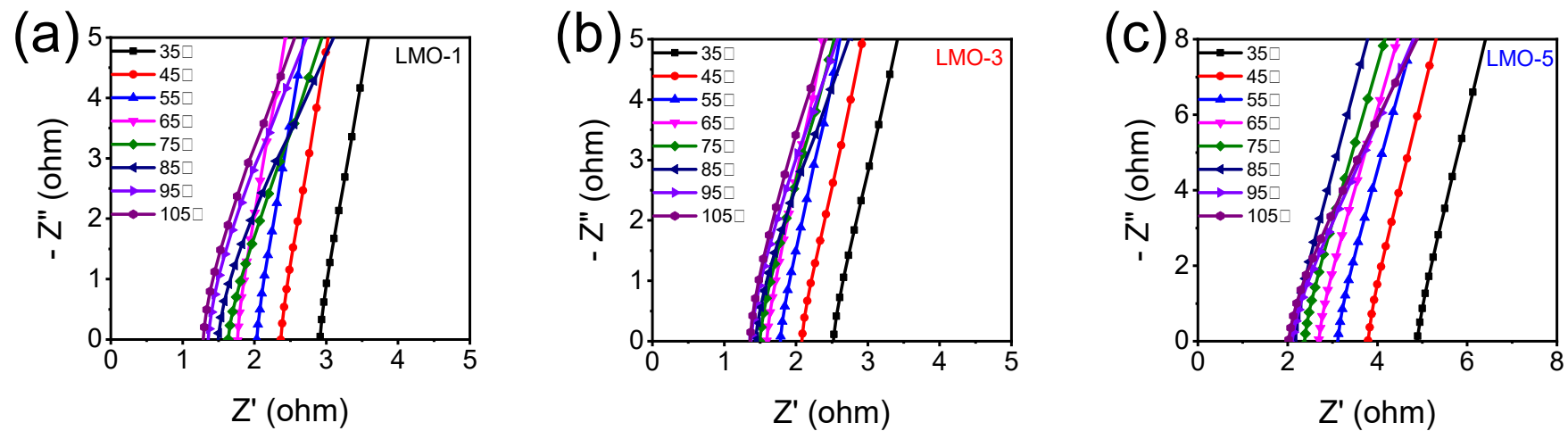


Figure S5. EIS test of LMO-1 (a), LMO-3 (b), LMO-5 (c) in SS||SS cells under different temperatures.



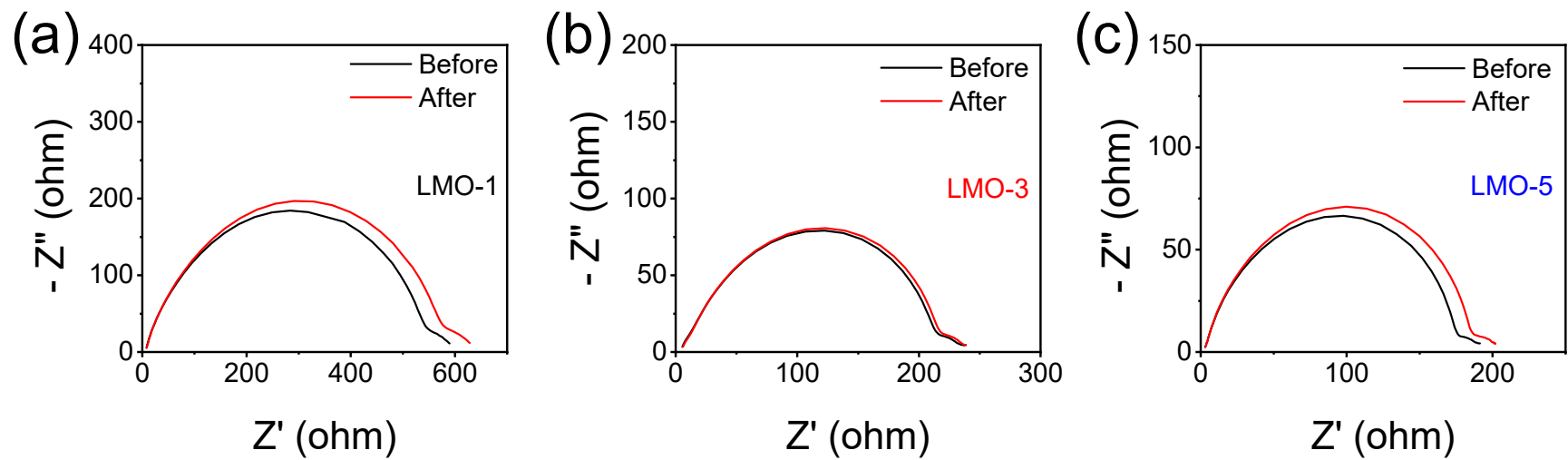


Figure S6. Impedance plots before and after  $\text{Li}^+$  transfer number test.

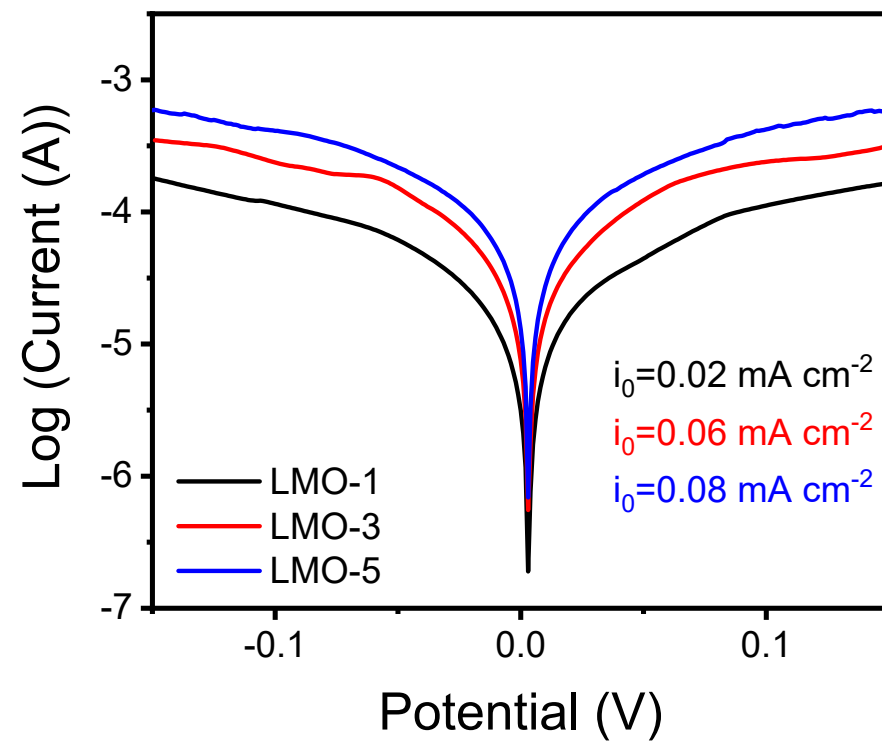


Figure S7. Tafel plots of symmetric cell Li|LMO-X|Li.

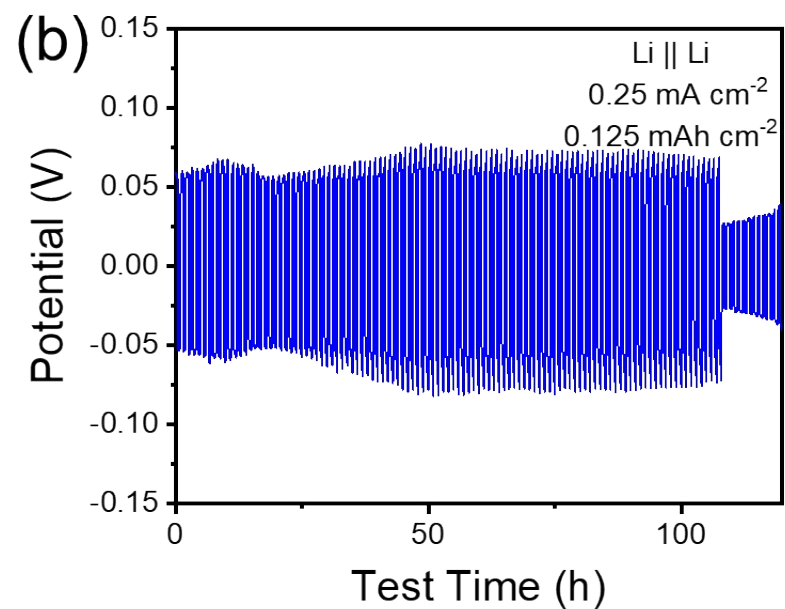
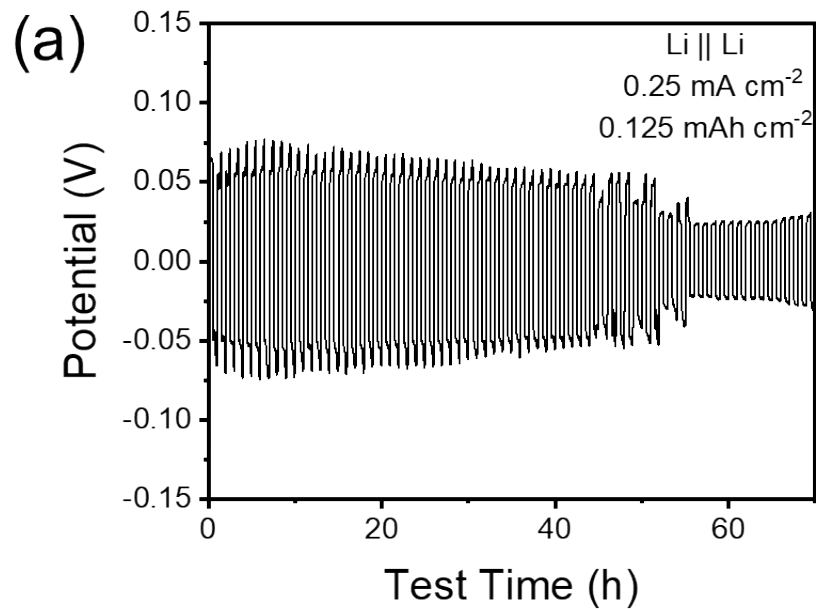


Figure S8. Galvanostatic cycling of lithium symmetric cells applying LMO-1 (a) and LMO-5 (b) in under 0.25 mA cm<sup>-2</sup> to reach 0.125 mAh cm<sup>-2</sup>.

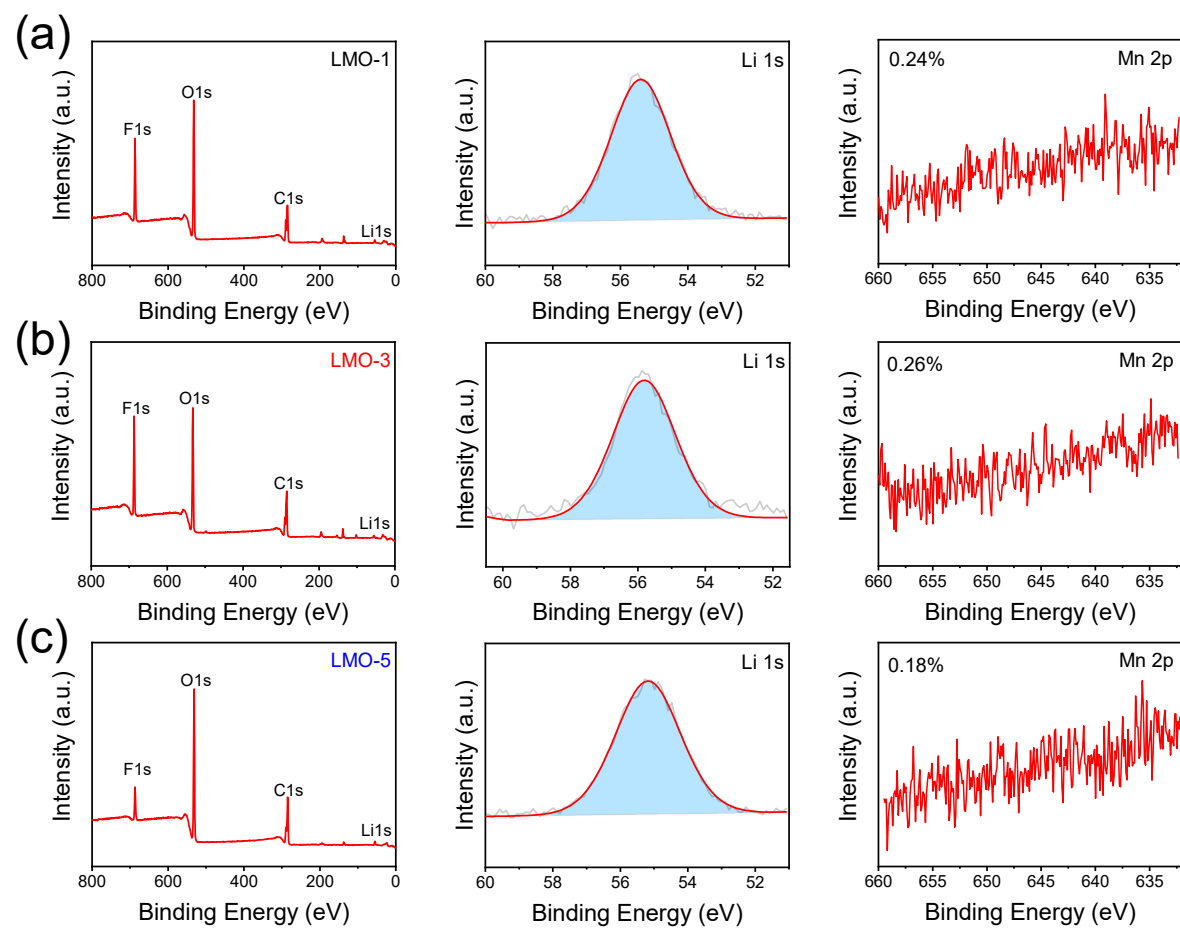


Figure S9. XPS profiles of Li||Li symmetric cells after cycling under  $0.25 \text{ mA cm}^{-2}$  and  $0.125 \text{ mAh cm}^{-2}$  with varying SSEs. (a) LMO-1, (b) LMO-3, and (c) LMO-5.

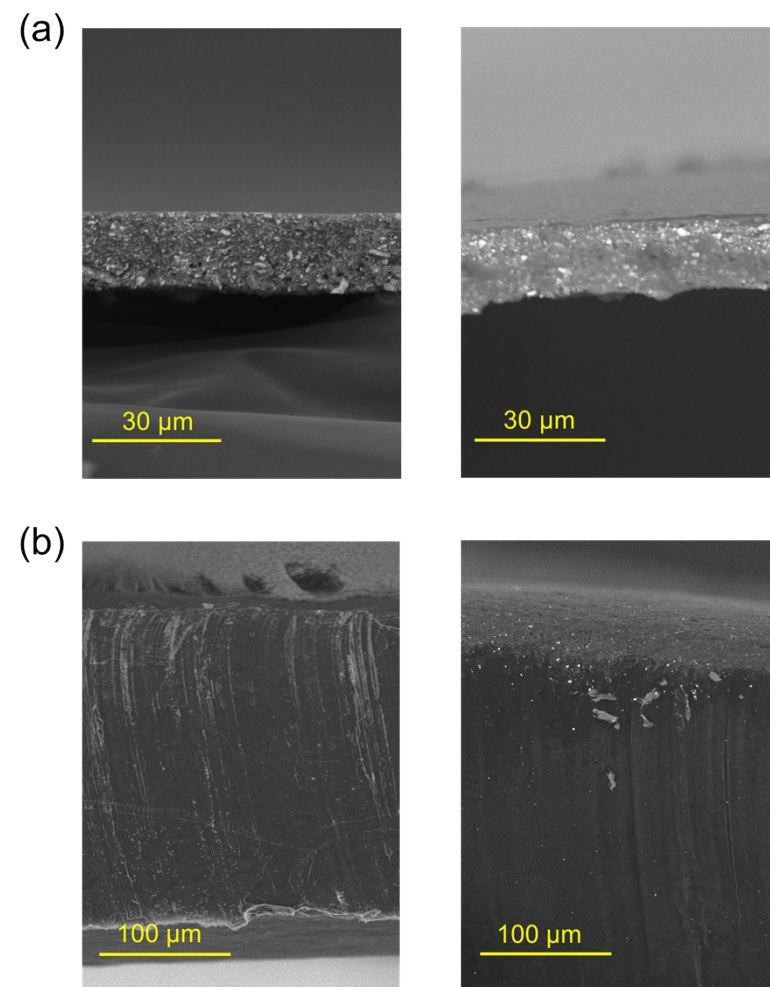


Figure S10. Cross-section SEM images of Li|LMO-3|Li symmetric cell before and after cycling under  $0.25 \text{ mA cm}^{-2}$  and  $0.125 \text{ mAh cm}^{-2}$ . (a) LMO-3 and (b) Li anode metal.

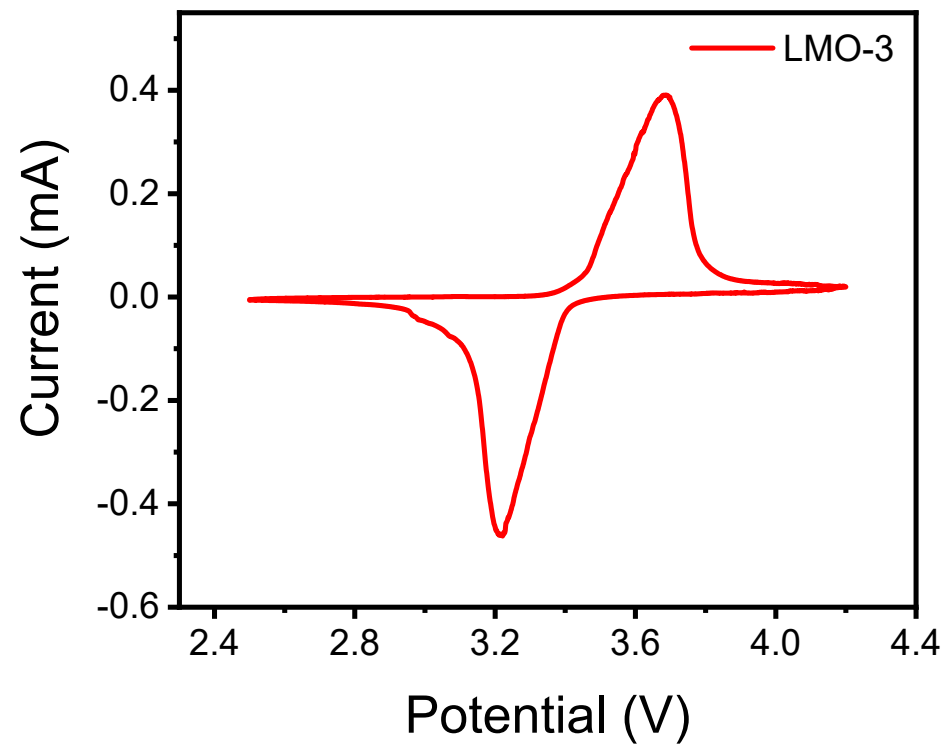


Figure S11. Cyclic voltammety curve of the Li|LMO-3|LFP cell.

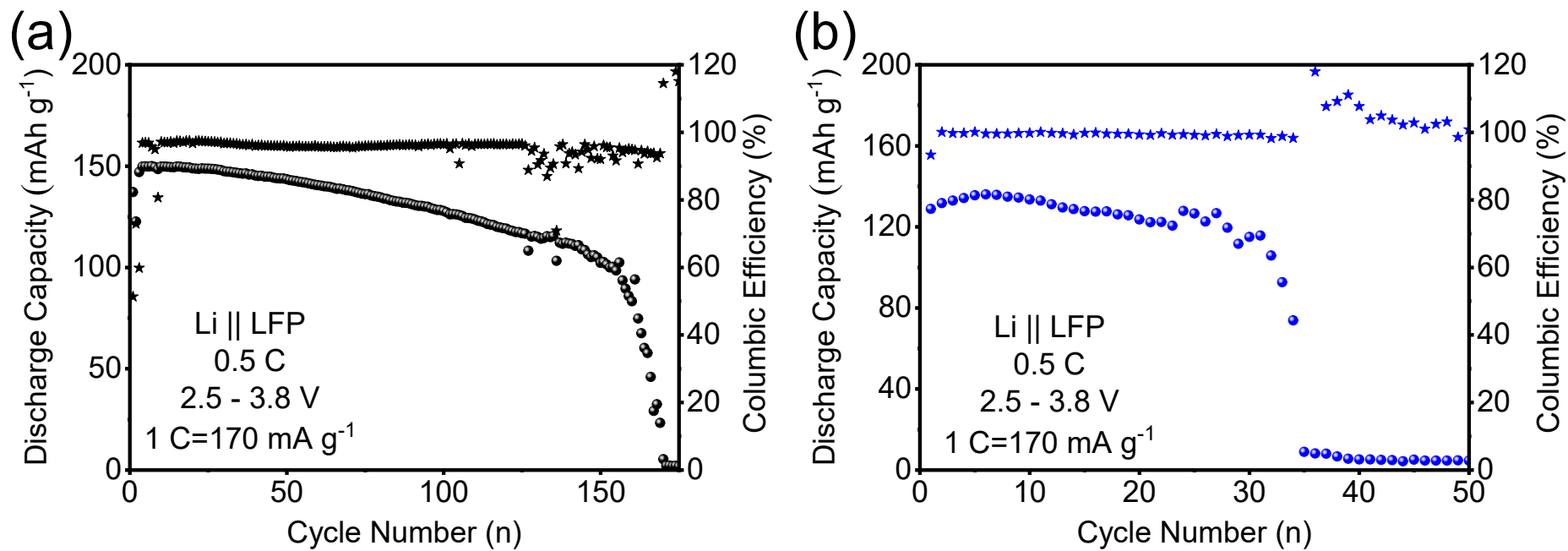


Figure S12. Cycling performance of Li||LFP cells with LMO-1 (a) and LMO-5 (b) at 0.5 C.

Table S1. The vibration modes corresponding to each infrared absorption peak.

<b>Absorption peak (cm<sup>-1</sup>)</b>	<b>Stretching vibration modes</b>
1401	CH <sub>2</sub> wagging vibration
1169	CF <sub>2</sub> asymmetric stretching vibration
873	C-C skeletal vibration
600, 563	MnO <sub>6</sub> asymmetric stretching vibration
479	CF <sub>2</sub> bending vibration



Table S2 Comparison of ionic conductivities and cycling performance for SSEs.

Solid State electrolyte	Thickness ( $\mu\text{m}$ )	Conductivity ( $\text{S cm}^{-1}$ )	Cathode material	Cycling performance	Ref.
PVDF/30 wt.% LMO	~20	$5.17 \times 10^{-4}$ at 35 °C	LFP	147.7 mAh $\text{g}^{-1}$ after 200 cycles under 0.5C at 35 °C	This work
PEO/VAVS/LiTFSI		$1.89 \times 10^{-4}$ at 25 °C	LFP	110.7 mAh $\text{g}^{-1}$ after 200 cycles under 0.5C at 35 °C	1
PE/SN/PEGDA/1% wt.%LiNO <sub>3</sub> /LiTFSI	~16	$1.08 \times 10^{-4}$ at room temperature	LCO	110.6 mAh $\text{g}^{-1}$ after 385 cycles under 0.2C at room temperature	2
PEO/ZiF-67/LiTFSI		$1.0 \times 10^{-4}$ at 25 °C	LFP	124.0 mAh $\text{g}^{-1}$ after 200 cycles under 0.2C at 60 °C	3
PEO/10 wt.% LLZO/LiTFSI	~40	$2.39 \times 10^{-4}$ at 25 °C	LFP	107.0 mAh $\text{g}^{-1}$ after 200 cycles under 0.1C at 60 °C	4
PEO/LiTFSI/wheat flour electrolyte	~300	$2.62 \times 10^{-5}$ at 25 °C	NCM811	62.9 mAh $\text{g}^{-1}$ after 60 cycles under 0.1C at 25 °C	5
PEO/10% SiO <sub>2</sub> /LiClO <sub>4</sub>	~200	$4.4 \times 10^{-5}$ at 30 °C	LFP	100.0 mAh $\text{g}^{-1}$ after 80 cycles under 0.1C at 60 °C	6
P(PO/EM)/LITFPFB		$1.55 \times 10^{-4}$ at 70 °C	LiFe <sub>0.2</sub> Mn <sub>0.8</sub> PO <sub>4</sub>	125.6 mAh $\text{g}^{-1}$ after 100 cycles under 0.1C at 70 °C	7
QSCE-PH/GPFIL3/P	~21	$3.24 \times 10^{-4}$ at room temperature	LFP	117.0 mAh $\text{g}^{-1}$ after 350 cycles under 0.5C at 30 °C	8
PEO/10 wt.% LLZTO/LiTFSI	~70	$1.17 \times 10^{-4}$ at 30 °C	LFP	127.0 mAh $\text{g}^{-1}$ after 200 cycles under 0.2C at 55 °C	9

1. W. Tang, S. Tang, X. Guan, X. Zhang, Q. Xiang and J. Luo, *Adv. Funct. Mater.*, 2019, **29**, 1900648.
2. B. Yuan, B. Zhao, Q. Wang, Y. Bai, Z. Cheng, Z. Cong, Y. Lu, F. Ji, F. Shen, P.-F. Wang and X. Han, *Energy Storage Mater.*, 2022, **47**, 288-296.
3. Y. Zou, Z. Ao, Z. Zhang, N. Chen, H. Zou, Y. Lv and Y. Huang, *Chem. Eng. Sci.*, 2023, **275**, 118705.
4. J. Zhang, N. Zhao, M. Zhang, Y. Li, P. K. Chu, X. Guo, Z. Di, X. Wang and H. Li, *Nano Energy*, 2016, **28**, 447-454.
5. Y. Lin, Y. Cheng, J. Li, J. D. Miller, J. Liu and X. Wang, *RSC Adv.*, 2017, **7**, 24856-24863.
6. D. Lin, W. Liu, Y. Liu, H. R. Lee, P. C. Hsu, K. Liu and Y. Cui, *Nano Lett.*, 2016, **16**, 459-465.
7. Q. Wang, Z. Cui, Q. Zhou, X. Shangguan, X. Du, S. Dong, L. Qiao, S. Huang, X. Liu, K. Tang, X. Zhou and G. Cui, *Energy Storage Mater.*, 2020, **25**, 756-763.
8. Y. Cui, G. Yu, R. Liu, D. Miao and D. Wu, *Chin. J. Chem.*, 2023, **41**, 2848-2854.
9. L. Chen, Y. Li, S.-P. Li, L.-Z. Fan, C.-W. Nan and J. B. Goodenough, *Nano Energy*, 2018, **46**, 176-184.